ISBN: 978-3-95450-247-9 ISSN: 2673-5490 doi: 10.18429/JACoW-IPAC2024-THPS22

DESIGN STUDY OF A COMPACT SUPERCONDUCTING UNDULATOR BASED ON LASER-STRUCTURED HTS TAPES

B. Krasch*, F. Abusaif, N. Glamann, A. Grau, R. Nast, D. Saez de Jauregui
Karlsruhe Institute of Technology (KIT), Karlsruhe, Germany

Abstract

Undulators serve as a source of X-ray radiation in synchrotron storage rings or in free-electron laser (FEL) facilities. Due to the requirement to build energy efficient accelerators of the next generation, undulators need to be further developed accordingly. The associated design of undulators with short period lengths (≤ 10 mm) and small magnetic gaps (≤ 4 mm) while maintaining small-scale high magnetic fields is only possible through the use of high-temperature superconductors (HTS). HTS tapes are suitable candidates, as they allow both high critical current densities and high critical magnetic fields at higher temperatures. KIT has therefore developed a new concept by structuring a meandering pattern on the surface of the HTS tapes with ps laser pulses. This type of surface structuring generates a quasi-sinusoidal current flow in the HTS tape. By stacking several tapes in a proper manner, the desired alternating dipole field is achieved.

In this work we present the results of our design study on the cooling concept of a compact HTS undulator.

INTRODUCTION

Insertion devices, such as undulators, are key components for free-electron laser (FEL) facilities and advanced synchrotron radiation sources, since they produce coherent photon beams with high brilliance and a wide spectral range. Through the commercial use of superconducting materials, the first superconducting undulators (SCU) were built. Compared to conventional cryogenic permanent magnets, SCUs provide a higher peak field on axis and thus a higher tunability and brightness for the same geometry [1], resulting in a wider range of applications at modern synchrotron light sources. The traditional technology of winding a low-temperature superconductor wire around a coil reaches its limits due to the natural expansion of the wire cross-section, making it difficult to realise period lengths ≤ 8 mm. Due to the requirement to build energy-efficient accelerators, new concepts have been developed to produce more compact undulators with even shorter wavelengths based on high temperature superconductors (HTS) [2–5]. The current developments of SCU technology in general is described here [6–8]. One promising approach by Prestemon et al. [9, 10] is the design of meander structured HTS tapes. Based on this idea, T. Holubek et al. [11] and A. Will et al. [12] developed different realisations which are currently further investigated at KIT. In both concepts laser pulses in the ps range are used for the meandering structuring process in order to avoid localised damage to the material due to overheating [13]. This type of structuring assumes that the current takes a sinusoidal path through the HTS tape and by stacking up to 30 layers of HTS on top of each other, the desired undulator dipole field is generated. In the jointless concept by T. Holubek [11], a single 15 m long tape is structured at regular intervals in such a way that winding it around a stainless steel yoke leads to a precise overlap . The zigzag concept by A. Will [12] uses 30 individual 25 cm long HTS tapes, each of which is soldered at one end to the tape above it. This results in an accordion-like arrangement. In order to achieve the alternating dipole magnetic field, the tapes must be stacked in an alternating current direction with a 180° phase shift between each two layers for both methods (jointless and zigzag). Advantages and disadvantages as well as the current status of the concepts can be found here [14, 15]. The cooling concept for such a compact HTS undulator is presented in the following sections, whereby the type of winding does not play a major role here.

COOLING CONCEPT

The cooling concept for a compact HTS undulator is a crucial step on the way to its realisation. At this point, the design of the vacuum chamber including current leads, cold shield and liner is presented. The following two restrictions were defined at the start of the design phase:

- Use of a liner to absorb beam heat loads, so that magnet coils are not affected.
- The cooling of the undulator is refrigerant-free (e.g. no liquid helium) and therefore cryocoolers are used.

LINER During the development process of the cooling concept, it was decided to use a liner for three reasons. First, all beam heat loads act on the liner, where they are cooled, rather than heating the HTS tape itself. Second, to minimise the influence of impedances on the electron beam. Third, the liner is a thin vacuum chamber that separates the vacuum of the cryostat $\left(10^{-6}\,\text{mbar}\right)$, where the magnet system is located, from that of the electron beam tube $\left(10^{-9}\,\text{mbar}\right)$, which means that the vacuum chamber does not have to be designed for ultra high vacuum (UHV). The main disadvantage is that the magnetic gap has to be higher, which reduces the magnetic field. The second disadvantage is that this vacuum chamber is an additional costly component to design, build, install and cool. The current design of the liner is cuboid, as shown on top in Fig. 2. The liner is mainly made of copper with a residual resistivity ratio (RRR) of at least 100 in order to keep the impedances low. The 0.3 mm thick stainless steel layer on the top and bottom serves to better stabilise the liner and to connect it to the vacuum chamber.

* bennet.krasch@kit.edu

ISBN: 978-3-95450-247-9 ISSN: 2673-5490 doi: 10.18429/JACoW-IPAC2024-THPS22

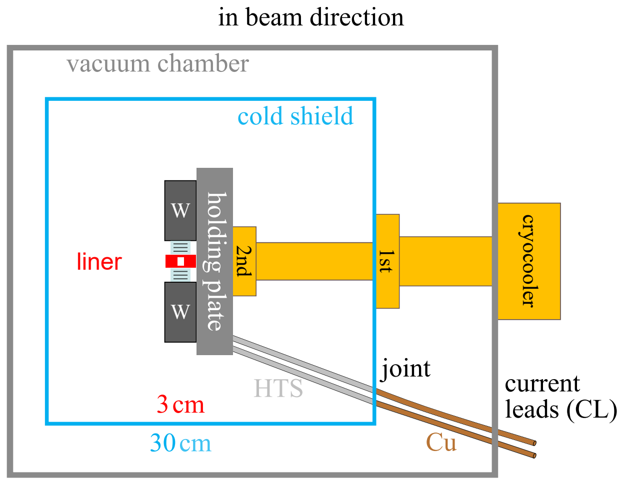

Figure 1: Design of the vacuum chamber. In the centre, the rectangular liner is shown in red. The 30 layer stacks of HTS tapes are above and below it and are fixed to the stainless steel yokes (W). The holding plate is mounted directly on the 2^{nd} cold stage of the CC. This arrangement is located inside the cold shield, which is connected to the 1^{st} stage of the CC. The current leads are shown here in simplified form without feed-through connectors.

CRYOSTAT Based on the two restrictions, Fig. 1 shows the cooling concept in simplified form. A two-stage Gifford-McMahon SRDK-415D cryocooler (CC) is used, which provides a power of 1.5 W at 4 K at its second cold stage[1]. The holding plate with the magnets is directly mounted on the 2^{nd} cold stage to guarantee the desired 4 K in order to be able to transport the maximum current through the HTS tapes. The liner is connected to the cold shield only via its front and rear side. The cold shield in turn is connected to the 1^{st} stage of the CC. This is where the advantage of the liner becomes clear, since it shields the magnets from heat loads, such as resistive wall heating caused by the electron beam. Therefore, more cooling capacity is needed, which is why the liner is connected to the 1^{st} cold stage, as a higher cooling capacity is available there at higher temperatures. This means that almost the entire cooling capacity of the CC's 2^{nd} cooling stage can be used for the undulator magnet. In addition, the liner is connected to the beam tube of a storage ring, which separates the two vacuum areas, that of the cryostat with the coils and the UHV area of the electron beam. The current lead (CL) is a hybrid (metal - HTS material), conduction-cooled CL. The metal part from the lid of the vacuum chamber to the joint is a copper strand (Cu) that is normal conductive. The joint is thermally connected to the 1^{st} stage of the CC. The HTS part of the CL, which is cooled by the 2^{nd} stage of the CC, is then connected to the joint.

STUDY ON HEAT LOADS In the first step, the individual sources of heat and their respective contributions are identified, see Table 1, so that, in the second step, the

[1] Capacity map SRDK-415D `https://www.shicryogenics.com/wp-content/uploads/2020/09/RDK-415D_Capacity_Map.pdf`.

Table 1: Heat Loads to the Cold Stages of the Cryocooler

Source of heat load	1^{st} stage (W)	2^{nd} stage (W)
Current leads (CL)	34	0.15
Instrumentation CL	0.05	-
Beam heat load	0.1	-
Thermal radiation	10	0.01
in total	**44.15**	**0.16**

temperature profile in the cryostat can be simulated for the 1^{st} cold stage (liner) and the 2^{st} cold stage (holding plate). As already described, a hybrid Cu-HTS **current lead** is used. For the 1^{st} cold stage, E. Shabagin [18] calculates the value of 42.5 W kA^{-1} as heat input for a single CL from from 300 K to 77 K. This is based on the assumption that it is an ideal CL with no additional heat load at the hot end. P. F. Herrmann et al. [19] calculated 41 W kA^{-1} for the metal part from 300 K to 77 K under the assumption of conduction cooling. As the structured HTS tapes are to be operated with a maximum current of 400 A, this results in a thermal load of 17 W resp. 16.4 W per CL and in a total of 34 W. The transition to the 2^{nd} cold stage is designed using HTS material. This input is mainly determined by the material and its cross-section. P. F. Herrmann et al. [19] use Bi-2212 and Y-123 tubes and obtain a heat load of 120 mW kA^{-1} resp. 320 mW kA^{-1}. For Bi-2223/AgAu strips, H. Zhang et al. [20] give a load of 100 mW at 650 A. Since the final HTS material has not been decided yet, 150 mW is therefore assumed as a compromise for two CLs.

The second item in Table 1 **instrumentation CL** includes temperature sensors on the Cu-HTS joint and sensors for quench detection. Based on experience, this value is conservatively set at 0.05 W.

The third item in Table 1 is **beam heat load**. Beam heat loads are caused by various heating mechanisms such as synchrotron radiation and impedances, whereby the latter is divided into geometric and resistive (also known as high frequency image currents or resistive wall (RW) heating). These effects depend to varying degrees on beam energy E, average beam current I, total number of bunches M, and bunch length σ_z. S. Casalbuoni et al. [16] calculated heat loads from synchrotron radiation (63 mW) and RW heating (22 mW) with respect to the typical standard parameter set at KARA for an undulator. Even if the geometry of the undulator does not completely match that of the compact HTS undulator, these values serve as a starting point for the subsequent simulation. D. Astapovych et al. [17] investigated numerically the heat load by RW heating and the geometric impedance for a compact HTS undulator as described above with 5 mm magnetic gap, 30 layers of structured HTS tapes and beam parameters as for KARA. D. Astapovych shows that geometric impedances increase towards higher frequencies and are of the same order of magnitude as RW heating at lower frequencies. Her detailed investigations indicate that the anomalous skin effect has an influence for RW

ISBN: 978-3-95450-247-9 ISSN: 2673-5490 doi: 10.18429/JACoW-IPAC2024-THPS22

heating that must be taken into account and that the impact of the structuring of the HTS tapes can be neglected. This simulation does not foresee a liner, which means that the RW heating acts directly on the silver layer of the HTS tape. Based on the simulation using CST Particle Studio, she obtains a value of 67 mW as a worse case scenario for the heat load through RW heating (conductivity of 2.01×10^9 S/m with RRR = 30). As the liner is made of Cu, a conductivity of 1.33×10^9 S/m at an RRR = 20 results in a corresponding heat load of 101 mW. Synchrotron radiation from the bending magnet can be neglected because a corresponding mask is mounted at the cryostat entrance, which prevents the synchrotron radiation from hitting the liner. The geometric impedance does not concern the liner, as in the design concept the tapering takes place outside the cryostat at room temperature. This means that the contribution from the RW heating with 0.1 W is the only beam load to be taken into account.

As the vacuum chamber is at room temperature, there is a heat input due to **thermal radiation**. Thermal convection can be neglected due to the vacuum (10^{-6} mbar), and also heat conduction, as there is no direct connection between the vacuum chamber and the cold shield. The value for thermal radiation is conservatively estimated using Stefan Boltzmann law $Q = \epsilon \sigma A T^4$. Following parameters were used: $T_{\text{chamber}} = 300\,\text{K}, T_{\text{shield}} = 30\,\text{K}, T_{\text{plate}} = 4\,\text{K}, A_{\text{chamber}} = 1.5\,\text{m}^2, A_{\text{shield}} = 0.66\,\text{m}^2, A_{\text{plate}} = 0.2\,\text{m}^2, \epsilon = 0.02$, the emission coefficient for polished stainless steel. $\sigma = 5.67 \times 10^{-8}\,\text{W/m}^2/\text{K}^4$ is the Stefan Boltzmann constant.

According to Table 1, a total of 0.16 W acts on the 2nd cold stage, which can be sufficiently cooled away with the 1.5 W at 4 K regarding the capacity map of the SRDK-415D. In order to compensate for the heat load of 55.16 W on the 1st cold stage, a temperature of around 70 K is reached in accordance with the capacity map. Since 70 K is too high a temperature for the liner, which is usually at 45 K at KARA, it is sufficient to use an additional single-stage CC. The RDK-400B, which provides around 50 W according to its capacity map[2], is suitable for this. In combination with the two-stage cryocooler, the liner should therefore be around 30 K.

COMSOL SIMULATION The heat inputs from Table 1 and the design of the cryostat, see Fig. 1, were used in the COMSOL Multiphysics software to obtain the temperature distribution along the liner and yokes. Since the temperature curve in the CC is not known and the corresponding capacity maps for certain temperatures at the cold stages indicate the available cooling capacity, the two cold stages are treated independently of each other. Figure 2 shows the dimensions of the liner at the top and the temperature distribution along the liner due to RW heating at the bottom. The temperature distribution on the support plate due to thermal radiation and CLs is shown in Fig. 3.

[2] Capacity Map of RDK-400B `https://www.shicryogenics.com/wp-content/uploads/2020/09/RDK-400B_Capacity_Map.pdf`.

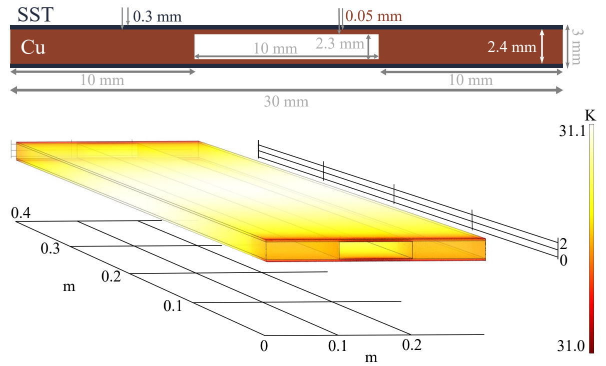

Figure 2: Dimensions and temperature distribution liner. The liner is cuboid with a rectangular base area of 30 mm wide and 3 mm high and mainly made by copper (Cu) with a 0.3 mm thin layer of stainless steel (SST) on top and bottom of the Cu block. The heat load by RW heating leads to an increase of 0.1 K in the centre of the liner.

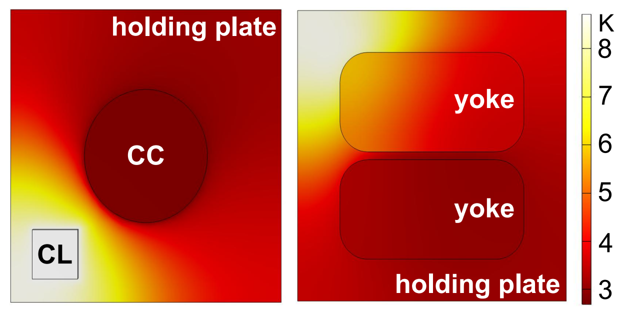

Figure 3: Temperature distribution holding plate. Left: The circle in the centre represents the CC and the square at the bottom left the CLs. It can be clearly seen that the area around the CLs is the warmest at 8 K. Right: The back shows the two yokes, whereby the upper heats up to 6 K. The area of the tapes heats up to a maximum of 4 K.

SUMMARY AND OUTLOOK

HTS tapes make it possible to build more compact and energy-efficient undulators. In this paper, the cooling concept of an HTS undulator was introduced. The advantages of a liner to absorb the beam heat loads were presented, followed by a detailed discussion of possible sources of heat loads. The CLs are the main reason why a second single-stage CC is provided in addition to the two-stage CC. The remaining beam load is RW heating with 0.1 W that is covered by the cooling power of the 2nd cold stage.

The next step will be to develop the cooling design in terms of tapering and integration into an existing cryostat.

ACKNOWLEDGEMENTS

The authors would like to thank Rainer Nast, KIT ITEP, for his continuous assistance in the fabrication of the laser-structured pattern on the tape surface.

This work was supported by the German Federal Ministry of Education and Research (BMBF) under the grant no. 05K19VK1.

ISBN: 978-3-95450-247-9 ISSN: 2673-5490 doi: 10.18429/JACoW-IPAC2024-THPS22

REFERENCES

[1] I. Kesgin *et al.*, "High-temperature superconducting undulator magnets", *Superconductor Science and Technology*, vol. 30, no. 4, pp. 04LT01, 2017. doi:10.1088/1361-6668/aa5d48

[2] S. Kim *et al.*, "Feasibility of a short-period superconducting undulator using 2G HTS tapes", *IEEE Transactions on Applied Superconductivity*, vol. 21, no. 3, pp. 1709 - 1712, 2017. doi:10.1109/TASC.2010.2089030

[3] S. Casalbuoni *et al.*, "High temperature superconducting tapes for undulator technology", *Superconductor Science and Technology*, vol. 30, no. 7, pp. 070501, 2017. doi:10.1088/1361-6668/aa6f63

[4] M. Calvi *et al.*, "GdBCO bulk superconducting helical undulator for x-ray free-electron lasers", *Physical Review Research*, vol. 5, iss. 3, pp. L032020, 2023. doi:10.1103/PhysRevResearch.5.L032020

[5] K. Zhang *et al.*, "Record field in a 10 mm-period bulk high-temperature superconducting undulator", *Superconductor Science and Technology*, vol. 36, no. 5, 2023. doi:10.1088/1361-6668/acc1a8

[6] K. Zhang *et al.*, "Review and prospects of world-wide superconducting undulator development for synchrotrons and FELs", *Superconductor Science and Technology*, vol. 35, no. 9, pp. 093001, 2022. doi:10.1088/1361-6668/ac782a

[7] V. Grattoni and S. Casalbuoni, "Design study for HybriSCU: A nybrid NbTi/ReBCO superconducting undulator", *IEEE Transactions on Applied Superconductivity*, vol. 33, no. 5, pp. 1-5, 2023. doi:10.1109/tasc.2023.3259329

[8] S. Casalbuoni *et al.*, "Superconducting undulator activities at the European X-ray free-electron laser facility", *Frontiers Media SA*, vol. 11, 2023. doi:10.3389/fphy.2023.1204073

[9] S. Prestemon *et al.*, "High performance short-period undulators using high temperature superconductor tapes", in *Proc. PAC'09*, Vancouver, Canada, paper WE5RFP075, pp. 2438–2440, 2010.

[10] S. Prestemon *et al.*, "Development and analysis of HTS undulator components for FEL applications", *IEEE transactions on applied superconductivity*, vol. 21, no. 3, pp. 1880-1883, 2013. doi:10.1109/TASC.2010.2098014

[11] T. Holubek *et al.*, "A novel concept of high temperature superconducting undulator", *Superconductor Science and Technology*, vol. 30, no. 11, p. 115002, 2017. doi:10.1088/1361-6668/aa87f1

[12] A. Will *et al.*, "Design and Fabrication Concepts of a Compact Undulator with Laser-Structured 2G-HTS Tapes", in *Proc. IPAC'21*, Campinas, Brazil, May 2021, pp. 3851–3854. doi:10.18429/JACoW-IPAC2021-THPAB048

[13] R. Nast *et al.*, "Influence of laser striations on the properties of coated conductors", *Journal of Physics: Conference Series*, vol. 507, no. 2, pp. 022023, 2014. doi:10.1088/1742-6596/507/2/022023

[14] D. Astapovych *et al.*, "Magnetic field investigation in a compact superconducting undulator with HTS tape", *International Free Electron Laser Conference (FEL)*, Triest, Italien, 2022. doi:10.5445/IR/1000153873

[15] B. Krasch *et al.*, "Measurement setup and magnetic field studies of a compact superconducting undulator with laser-structured HTS tapes", *IEEE Transactions on Applied Superconductivity*, vol. 34, no. 5, pp. 1-4, 2024. doi:10.1109/TASC.2024.3355320

[16] S. Casalbuoni *et al.*, "Beam heat load and pressure rise in a cold vacuum chamber", *Physical Review ST Accelerators and Beams*, vol. 10, no. 9, pp. 093202, 2007. doi:10.1103/PhysRevSTAB.10.093202

[17] D. Astapovych *et al.*, "Investigation of Beam Impedance and Heat Load in a High Temperature Superconducting Undulator", in *Proc. IPAC'21*, Campinas, Brazil, May 2021, pp. 2089–2092. doi:10.18429/JACoW-IPAC2021-TUPAB267

[18] E. Shabagin, "Development of a CMRC cooled 10 kA current lead for HTS applications", Karlsruhe Institute of Technology, Phd thesis, 2022. doi:10.5445/IR/1000144514

[19] P. F. Herrmann *et al.*, "Cryogenic load calculation of high Tc current lead", *Cryogenics*, vol. 33, no. 5, pp. 555 - 562, 1993. doi:10.1016/0011-2275(93)90253-k

[20] H. Zhang *et al.*, "Design and experiment of conduction cooling HTS current leads suited for superconducting Wiggler magnets", *Physica C: Superconductivity and its Applications*, vol. 618, pp. 1354433, 2024. doi:10.1016/j.physc.2023.1354433